

Observation of Andreev Reflection Enhanced Shot Noise

P. Dieleman*, H.G. Bokkems, T.M. Klapwijk

Department of Applied Physics and Materials Science Center, University of Groningen, Nijenborgh 4, 9747 AG Groningen, The Netherlands

M. Schicke, and K.H. Gundlach

Institut de Radio Astronomie Millimétrique, 300 Rue de la Piscine, Domaine Universitaire de Grenoble, 38406 St. Martin d'Hères, France.

We have experimentally investigated the quasiparticle shot noise in NbN/MgO/NbN superconductor - insulator - superconductor tunnel junctions. The observed shot noise is significantly larger than theoretically expected. We attribute this to the occurrence of multiple Andreev reflection processes in pinholes present in the MgO barrier. This mechanism causes the current to flow in large charge quanta (*Andreev clusters*), with a voltage dependent average value of $m \approx 1 + \frac{2\Delta}{eV}$ times the electron charge. Because of this charge enhancement effect, the shot noise is increased by the factor m .

PACS numbers: 72.70.+m, 74.50.+r, 74.80.Fp

A dc current I flowing through a vacuum tube or a tunnel junction generates shot noise, time dependent fluctuations of the current due to the discreteness of charge carriers. Shot noise studies provide information on the nature of conduction not obtainable by conductance studies, e.g. the electric charge of carriers or the degree of correlation in the conducting system. For an uncorrelated system in which the electrons do not interact, the passage of carriers can be described by a Poisson distribution. The spectral density of current fluctuations S_I then equals full shot noise: $S_I = 2qI = P_{\text{Poisson}}$ for zero frequency and temperature¹. The charge quantum q is normally the electron charge e .

In superconductor - normal metal (SN) systems Andreev reflection occurs, causing an effective charge to be transferred of $2e$. Due to this doubling of the charge, the shot noise in such a system is predicted to have a maximum of twice the Poisson noise²⁻⁴. More recently, giant shot noise in the supercurrent is predicted in a single-channel superconductor - normal metal - superconductor (SNS) point contact⁵ which is attributed to transport of large charge quanta ($q \gg e$) at finite voltages caused by Multiple Andreev Reflection (MAR)⁶. Observation of enhanced charge quanta in SN or SNS structures requires a combination of conductance and shot noise measurements. Despite extensive theoretical work, experimental results in this field are rare. A recent experiment⁷ is performed on a NbN/c/Nb structure in which c is assumed to be a Nb constriction with a length of 7 nm and a diameter of 15 nm. At 9.5 K the structure acts like an NS interface but doubled shot noise is not observed. The predicted giant supercurrent shot noise is not observed either (at 4.2 K).

From an applied point of view, shot noise in superconducting structures is of interest since this noise forms a major limitation to the sensitivity of NbN/MgO/NbN Superconductor-Insulator-Superconductor (SIS) THz radiation detectors⁸.

For these reasons, we have investigated quasiparticle current transport and shot noise in an SNS structure in which the quasiparticle current is carried by MAR. Anticipating the experimental shot noise results presented in this paper we demonstrate that *in a system in which multiple Andreev reflections occurs the quasiparticle shot noise at $V < 2\Delta/e$ has a maximum value given by $S_I = (1 + \frac{2\Delta}{eV})2eI$ because current is effectively carried by multiply charged quanta*. The maximum shot noise is obtained if the transmission probability of the system approaches zero³.

The structure under study consists of a NbN/MgO/NbN SIS tunnel junction with small defects in the 1 nm thick MgO barrier acting as parallel SNS point contacts. Commonly used Nb/AlO_x/Nb tunnel junctions are known to exhibit very low subgap "leakage" current because the barrier is formed by thermal oxidation of a thin Al layer which wets the Nb surface. For NbN junctions such a thermal oxidation process is not yet established. Currently the best results are obtained by direct deposition of the barrier material⁹, and defects occur due to "missing atoms" since the barrier is comprised of merely 1 - 2 atomic layers in high current density junctions¹⁰. In Fig. 1 the nearly perfect tunneling I, V characteristic of a Nb junction is compared with that of a typical NbN junction. Both are measured at 4.2 K. The NbN junction area is $0.8 \mu\text{m}^2$, the normal resistance R_N is 25Ω , the gap voltage $2\Delta/e$ is 4.8 mV. The Nb junction has an area of $1 \mu\text{m}^2$, a normal resistance R_N of 56Ω and a gap voltage of 2.8 mV. Clearly the subgap current of the NbN junction is much larger than the current in the Nb junction. In addition the subharmonic gap structure in the NbN I, V and dV/dI curves indicates that the subgap current is predominantly carried by MAR⁶. Since MAR is evidence for the presence of higher order processes¹¹ the observation of MAR indicates conducting paths with transmissivities close to 1, which we further call pinholes.

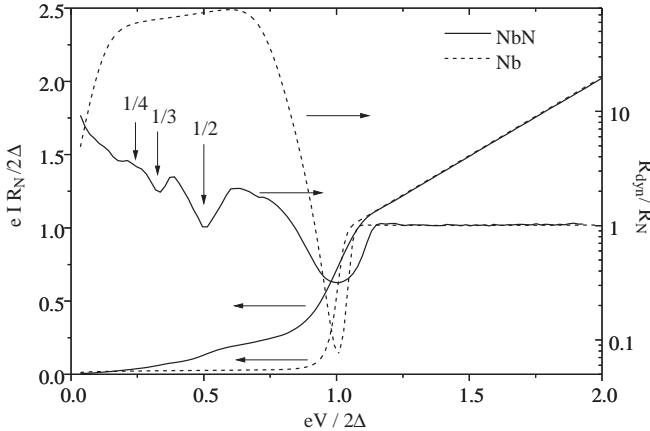


FIG. 1. Normalized I , V and $R_{dyn} = dV/dI$ curves of a Nb and NbN junction. The subgap structure is clearly visible up to the fourth harmonic in the NbN R_{dyn} curve.

A remarkable feature of a pinhole system is that varying the barrier thickness changes only the number of pinholes without affecting the pinhole conductance¹⁰. Therefore the pinholes can be considered as reproducible barrier defects with identical transmission probabilities. From the relative height of the current steps at the subharmonic gap structure in Fig. 1 a pinhole transmission probability T of 0.17 is derived¹¹. The supercurrent (Fraunhofer) dependence on magnetic field is nearly ideal, indicating a large number of pinholes with a homogeneous distribution over the barrier. All measured high current density NbN/MgO/NbN junctions exhibit similar behavior.

The noise measurement setup is schematically depicted in Fig. 2.

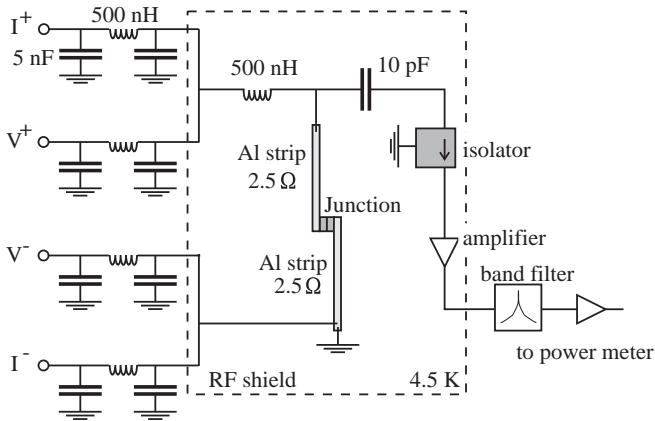


FIG. 2. Schematic layout of the current-voltage and noise measurement system. All leads going into the dewar are low-pass filtered except for the 1.5 GHz wiring. The Al leads suffice as heat sink.

All DC leads are filtered, 30Ω manganin wires carry currents between room temperature parts and those at cryogenic temperatures. The isolator is used to dissipate power reflected off the amplifier into a 50Ω load in or-

der to avoid gain variations with varying junction output impedance. A band pass filter transmits an 85 MHz band centered at 1.5 GHz. Although a spectrum of the signal was not taken, we assume the measured noise to be white since 1.5 GHz is high enough to ignore $1/f$ noise of the device.

The total gain of the amplification section is measured by mounting the high quality Nb SIS junction shown in Fig. 1 in the measurement setup. Since the Nb junction exhibits single particle tunneling, the shot noise generated by the current in the junction can be accurately calculated from the I , V curve¹². Corrections due to the measurement frequency of 1.5 GHz are negligible for voltages $V \gg \hbar\omega \approx 0.05$ mV. The effect of finite temperature below 0.5 mV is taken into account by using $S_I = 2eI \coth(eV/2k_B T)$ to calculate the noise coming from the junction. Comparing this noise with the noise power after filtering and amplification gives the total gain as well as the noise added by the isolator, cables and amplifier. The output power is given by¹²

$$P_{out} = G_{amp}B \left(\frac{1}{4}S_I R_{dyn}(1 - \Gamma^2)G_{iso} + k_B T \Gamma^2 \right) + k_B(1 - G_{iso})T + P_{amp} \quad (1)$$

in which G_{amp} is the amplifier gain, B is the bandwidth, I , V and R_{dyn} are the current, voltage and the differential resistance dV/dI of the junction, Γ is the reflection coefficient $|R_{dyn} - R_{amp}|/(R_{dyn} + R_{amp})$, G_{iso} is the isolator gain, and P_{amp} stands for the output noise of the amplifier chain. From the measured and calculated noise power curves the gain and noise of the amplifier and isolator can be accurately determined¹³ using Eq. 1. The loss of the isolator plus cables is 0.25 dB. The total amplification including cable losses and reflections is 80 dB.

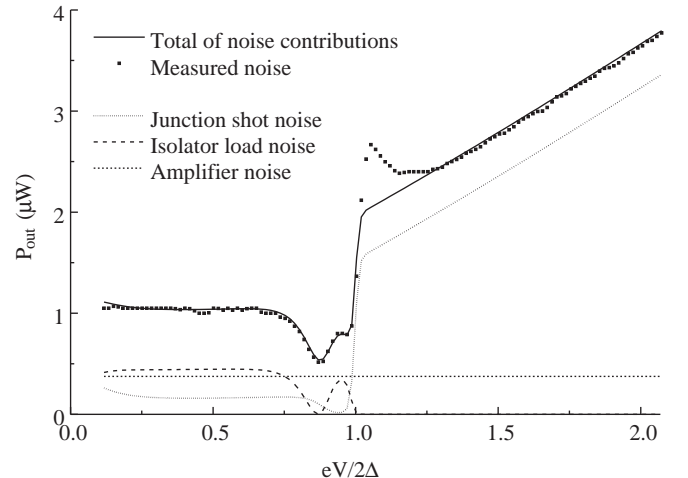


FIG. 3. Contributions of the Nb junction, isolator, and amplifiers to the total output noise. The measured total noise power is accurately given by Eq. 1. The deviation above the gap voltage may be connected to a proximity effect layer near the tunnel barrier causing doubled shot noise.

The shot noise S_I generated in the NbN junction is obtained by performing a measurement of P_{out} , I and dI/dV as function of voltage similar to that conducted for the Nb junction. Since the loss and gain of each component is known, the shot noise S_I can be derived from the output noise P_{out} using Eq. 1. The result is plotted in Fig. 4 together with the Poisson shot noise $2eI$ calculated using the measured I, V curve. The shot noise is expressed as a current by dividing the measured S_I by $2e$ to allow easy comparison with the shot noise calculated from the I, V curve. If the junction behaves as an ideal shot noise source as the Nb junction does, a comparison of $S_I/2e$ with the dc current I will find them identical at voltages above 0.5 mV. Clearly, below the gap voltage the measured noise is much larger than Poisson noise.

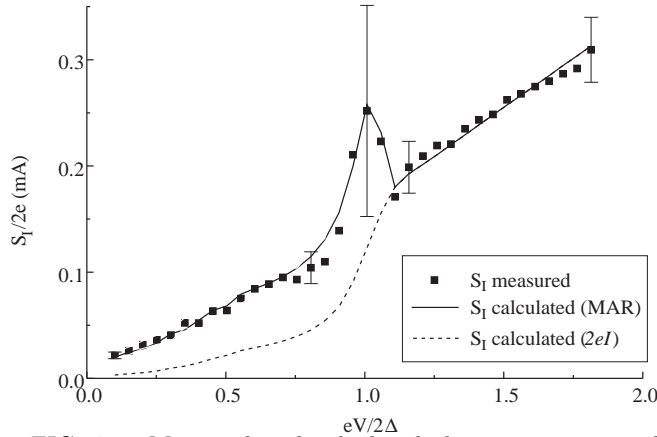


FIG. 4. Measured and calculated shot noise generated by the NbN junction, all normalized to current by division by $2e$. The square dots give the measured noise, the dashed line is the calculated Poisson shot noise curve. The calculation of the S_I curve labeled (MAR) is explained in the text. Above the gap voltage the shot noise follows Poisson noise since current transport through the barrier dominates. The error bars, given at specific points to avoid crowdedness of the figure, reflect the uncertainty in the noise contributions of the measurement equipment. Errors at intermediate voltage values can be roughly linearly interpolated. Offsets in current and noise are negligible since at negative voltage bias the same results are obtained.

We explain this excess noise by taking into account multiple Andreev reflection processes in the pinholes. For an NS structure with a disordered region of length L which is much smaller than the mean free path l in this region, the shot noise at $V \ll \Delta/e$ is given by:³

$$P_{NS}(T) = \frac{8(1-T)}{(2-T)^2} \cdot P_{\text{Poisson}} \quad (2)$$

in which T is the transparency of the barrier between the normal- and superconducting region. For $T \ll 1$ $P_{NS} = 2P_{\text{Poisson}}$ indicating uncorrelated current of particles with charge $2e$ due to Andreev reflection. Realizing that via multiple Andreev reflection much larger charge

quanta can be transferred⁵, the shot noise generated in pinholes by MAR is derived in the following way. The pinhole is assumed to consist of two SN and NS structures in series. If the measured transmission probability of 0.17 is inserted into Eq. 2 the shot noise suppression is a mere 1 %, below the measurement accuracy. Therefore if the effectively transferred charge q is known, the shot noise is simply found from $S_I = 2qI$. We calculate the charge $q(V)$ in the limit of unity pinhole transmission probability using the trajectory method employed in the original paper on MAR⁶. This enables separate calculation of the currents I_m carried by m Andreev reflections. The I_m values form weight factors used to calculate the average transferred charge carried by what might be called *Andreev clusters*.

The total current flowing from the left superconductor (at voltage V) to the right superconductor (at zero voltage) is given by the difference of⁶

$$I_{\text{LR}} = \frac{1}{eR_0} \int_{-\infty}^{\infty} dE f_0(E - eV) [1 - A(E - eV)] \cdot [1 + A(E) + A(E)A(E + eV) + \dots] \quad (3)$$

and

$$I_{\text{RL}} = \frac{1}{eR_0} \int_{-\infty}^{\infty} dE f_0(E) [1 - A(E)] \cdot [1 + A(E - eV) + A(E - eV)A(E - 2eV) + \dots] \quad (4)$$

where R_0 is the total normal state resistance of the pinholes, $f_0(E)$ is the Fermi distribution and $A(E)$ is the energy dependent Andreev reflection probability. The first term $[1 - A]$ denotes the fraction of available electrons in the superconductor which is transmitted into the normal region. The last term $[1 + \dots]$ gives the transferred charge multiple which is $1e$ if no Andreev reflections take place, $2e$ for one Andreev reflection, and so on. The currents I_m ($m = 1, 2, \dots$) carried by m -electron processes are calculated by splitting Eqs. 3 and 4 into the m -electron parts. For example I_2 is given by

$$I_2(V) = \frac{2}{eR_0} \int_{-\infty}^{\infty} dE \left(f_0(E - eV) [1 - A(E - eV)] \cdot A(E) [1 - A(E + eV)] - f_0(E) [1 - A(E)] A(E - eV) [1 - A(E - 2eV)] \right) \quad (5)$$

Since the current I_m is carried only by carriers with an m -fold charge, the magnitude of this current divided by the total current gives the relative contribution to the average transferred charge. Therefore the average charge q of an *Andreev cluster* for a given voltage V is given by:

$$q(V) = \frac{\sum_{m=1}^{\infty} m \cdot I_m(V)}{\sum_{m=1}^{\infty} I_m(V)} \cdot e \quad (6)$$

The resulting charge-voltage curve is shown in Fig. 5 and is used to calculate the noise $S_I = 2q(V)I$ in Fig. 4. The measured charge values in Fig. 5 are obtained by dividing the measured shotnoise by $2eI$. The similarly derived unity charge of the Nb junction is shown for comparison. The effect of finite temperatures on the shot noise correction factor $\coth(eV/2k_B T)$ at voltages $V \ll 2\Delta/e$ is negligible since $\coth(q(V)V/2k_B T) \approx \coth((1 + \frac{2\Delta}{eV}) \cdot \frac{eV}{2k_B T}) \approx \coth(\frac{\Delta}{k_B T}) \approx 1$.

Apart from a superposed subharmonic gap structure the effective NbN charge is proportional to $1/V$. This can be appreciated by performing the charge calculation ignoring Andreev reflection for energies $|E| > \Delta$. Higher order terms vanish and the average charge is equal to the charge quantum transferred; $q_n = ne$ at voltages $V_n = \frac{2\Delta}{n-1}$ for $n = 2, 3, \dots$ giving an analytical approximation $q(V) = e + \frac{2\Delta}{V}$.

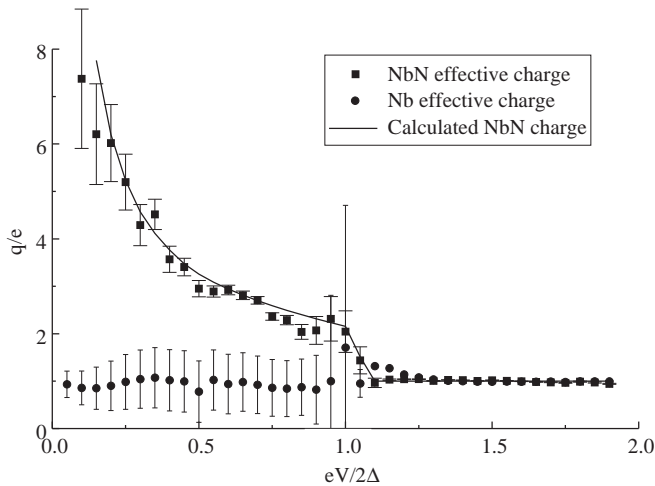


FIG. 5. Effective charge as function of voltage. The square dots give the charge derived from the measurements. The calculated charge values are used to calculate the shot noise in Fig. 4. For comparison the effective charge of the Nb calibration junction is shown by circles.

In conclusion, for the first time shot noise much larger than Poisson noise is observed in an SIS structure. A NbN SIS tunnel junction with pinholes is employed to obtain current transport dominated by multiple Andreev reflections (MAR). Due to the occurrence of MAR large charge quanta are transferred between the electrodes, causing a significantly enhanced shot noise. A simple model is developed to calculate the effective charge from which the shot noise is obtained. The model answers the question about the origin of excess noise in NbN⁸ and very high current density Nb¹⁴ SIS junctions in THz applications.

Note added in proof. After submission of this manuscript we became aware of theoretical work¹⁵ which analyzes MAR enhanced shot noise, in particular the dependence of S_I on temperature and transmission. In our semi-empirical theory we circumvent the problem of cal-

culating S_I by calculating $q(V)$ (ignoring coherence effects) and using the measured I .

We thank N. Whyborn for a remark initiating this work and N.B. Dubash for sharing his data and ideas. Helpful discussions and general assistance of S.G. den Hartog, B.J. van Wees, J.B.M. Jagers, J.R. Gao, H. Golsstein, H. van de Stadt, W. Hulshoff, D. Nguyen, and H.H.A. Schaeffer are acknowledged. This work is supported in part by the European Space Agency under contract No. 7898/88/NL/PB(SC) and the Stichting voor Technische Wetenschappen.

* Part of the work is performed at the Space Research Organisation of the Netherlands at Groningen, The Netherlands.

¹ D. Rogovin and D.J. Scalapino, *Ann. Physics* **68**, 1, (1974).

² V.A. Khlus, Sov. Phys. JETP **66**, 1243 (1987).

³ M.J.M. de Jong and C.W.J. Beenakker, Phys. Rev. B **49**, 16070 (1994).

⁴ B.A. Muzykantskii and D.E. Khmelnitskii, Phys. Rev. B **50**, 3982 (1994).

⁵ D. Averin and H.T. Imam, Phys. Rev. Lett. **76**, 3814 (1996).

⁶ T.M. Klapwijk, G.E. Blonder, and M. Tinkham, Physica **109-110B,C**, 1657 (1982).

⁷ Y. Misaki, A. Saito, and K. Hamasaki, Jpn. J. Appl. Phys. **36**, 2B 1190 (1996), Y. Misaki, A. Saito, S. Anezaki, and K. Hamasaki, unpublished.

⁸ P. Dieleman, T.M. Klapwijk, H. van de Stadt, *Eighth Int. Symp. on Space THz Techn.*, March 1997, Harvard University, Cambridge, MA, USA.

⁹ A. Shoji, M. Aoyagi, S. Kosaka, F. Shinoki, and H. Hayakawa, Appl. Phys. Lett. **46**, 1098 (1985).

¹⁰ A.W. Kleinsasser, R.E. Miller, W.H. Mallison, and G.B. Arnold, Phys. Rev. Lett. **72**, 1738 (1994).

¹¹ N. van der Post, E.T. Peters, I.K. Yanson, and J.M. van Ruitenbeek, Phys. Rev. Lett. **73**, 2611 (1994).

¹² N.B. Dubash, G. Pance, and M.J. Wengler, *IEEE Trans. Microwave Theory Tech.*, **42**, 715, (1994).

¹³ C.E. Honingh, J.J. Wezelman, M.M.T.M. Dierichs, G. de Lange, H.H.A. Schaeffer, T.M. Klapwijk, and M.W.M. de Graauw, *J. Appl. Phys.*, **74**, 4762 (1993).

¹⁴ G. de Lange, C.E. Honingh, J.J. Kuipers, H.H.A. Schaeffer, R.A. Panhuyzen, T.M. Klapwijk, H. van de Stadt, and M.W.M. de Graauw, *Appl. Phys. Lett.*, **64**, 3039 (1994).

¹⁵ J.P. Hessling, M.Sc. thesis, Chalmers, 1996. See further Report No. cond-mat 9509018.